Methodologies to Evaluate Simulations of Cardiac Tissue Abnormalities at a Cellular Level

Nicos Maglaveras and Ioanna Chouvarda

Aristotle University, The Medical School, Lab of Medical Informatics,
Box 323, 54124, Thessaloniki, Greece
{nicmag,ioanna}@med.auth.gr

Abstract. Computer Simulations of cardiac wave propagation may be used as a tool towards understanding the mechanisms of cardiac conduction, the nature of various heart diseases, as well as the effect of drugs in cardiac function. Such simulations depend on the ionuc current model adopted, and various such models have been proposed. The exact propagation wavefront thus depends on the ionic model and the tissue properties, being homogeneous or heterogeneous. The latter case, which corresponds to infracted cardiac tissue, is the focus in this work. The ionic current properties and the sodium kinetics on a two-dimensional grid where wavefront rotations around barriers at bifurcation sites take place, are examined in detail and differences in propagation characteristics elicited by using fast or slow fast inward current kinetics such as can be found in the Beeler-Reuter, Luo-Rudy and Ebihara-Johnson models are elaborated.

Keywords: ionic current models, cardiac propagation, conduction abnormalities.

1 Introduction

Cardiac tissue has received lots of attention in previous years regarding modeling and simulation of its function in normal and abnormal situations. Cardiac tissue has a number of different types of cells related with functionally different parts, such as the atrium, the AV node, the ventricles and the SA node to name the most well known ones.

In most cases the modeling and simulation of the function of the cardiac tissue at the cellular level depends on detailed ionic current based models such as the Luo-Rudy (LR), Ebihara-Johnson (EJ), Beeler Reuter (BR) and DiFrancesco and Noble (DFN) to name a few of the most well known ones [1-3]. Studies on the underlying physiological characteristics of conduction and their effect to the measured electrical field either at the surface of the heart or at the body surface are found in the literature. Usually the most addressed topics are the ones linked with the fast upstroke characteristics or the ones linked with the dispersion of refractoriness and the global repolarisation properties of the cardiac muscle.

The type of the ionic current models used and the kinetics properties may have a profound effect even in the basic propagation characteristics in the cardiac muscle. In

V.G. Duffy (Ed.): Digital Human Modeling, HCII 2007, LNCS 4561, pp. 694–702, 2007.

this study we investigate the effects of different ionic current models used when simulating propagation in myocardial infracted cardiac tissue linked with zig-zag type pathways, especially at the bifurcation sites as can occur in infracted tissue.

Fast and Kleber [4] presented a review regarding the theoretical background relating impulse propagation to wavefront curvature and analysed the role of wavefront curvature in electrical stimulation, formation of conduction block, and the dynamic behavior of spiral waves. The effects of tortuosity, created by spatial distribution of dead cell barriers, on 2-D propagation have been also studied by Maglaveras et al [5].

In this work, considering a rotating propagation wave, due to dead cell barriers, we take a closer look at the model kinetics in the area of rotation. The behavior of three ionic current models in such areas is compared. We show that the changes in ionic current spatial properties largely depend on the type of model of the fast inward current used, something that can be linked as well with the extracellular fields calculated at these sites, which may effect the correct identification of the activation instant when analyzing the electrograms.

2 Methods

2.1 The Ionic Current Models

The ionic current models used were the Beeler-Reuter (BR), Luo-Rudy (LR) and Ebihara-Johnson (EJ) [1-3]. The BR and LR in the fast inward current (I_{na}) formulation exhibit one activation gating variable (m) and two inactivation gating variables (h,j), while the EJ model exhibits one activation (m) and one inactivation (h) variable. The kinetics of the BR model are much slower when compared with the LR and EJ models, and this may play a role in the behaviour of the propagating wavefront especially in regions of high anatomical and functional complexity such as the bifurcation sites in an infracted cardiac tissue.

2.2 Data and Experimental Setup

Simulated data have been used for this work, in order to test and compare different methods for a structure of known complexity and behavior. Simulated experiments also allowed us to control the number of extracellular measurements to be used during the estimation procedure. The 2D monodomain model of cardiac muscle was used [5]-[6]. Signals are extracellular electrograms recorded at the surface of the tissue. A rectangular sheet of cells was simulated with a grid of 40x200 elements, which corresponds to 40x50 cells. Each cell consists of 4 longitudinal elements (3 cytoplasmic and 1 junctional). Elements were coupled by resistances. Beeler-Reuter Ebihara-Johnson and Luo-Rudy models have been used for ionic kinetics. These models express different kinetics, which lead to different frequency content. Regions of scar tissue were defined in order to introduce heterogeneity (see Figure 1). Simulation of propagation was implemented using Gauss Seidel method. The grid intervals were 10 μm transversely and 25 μm longitudinally and time step was 1μsec.

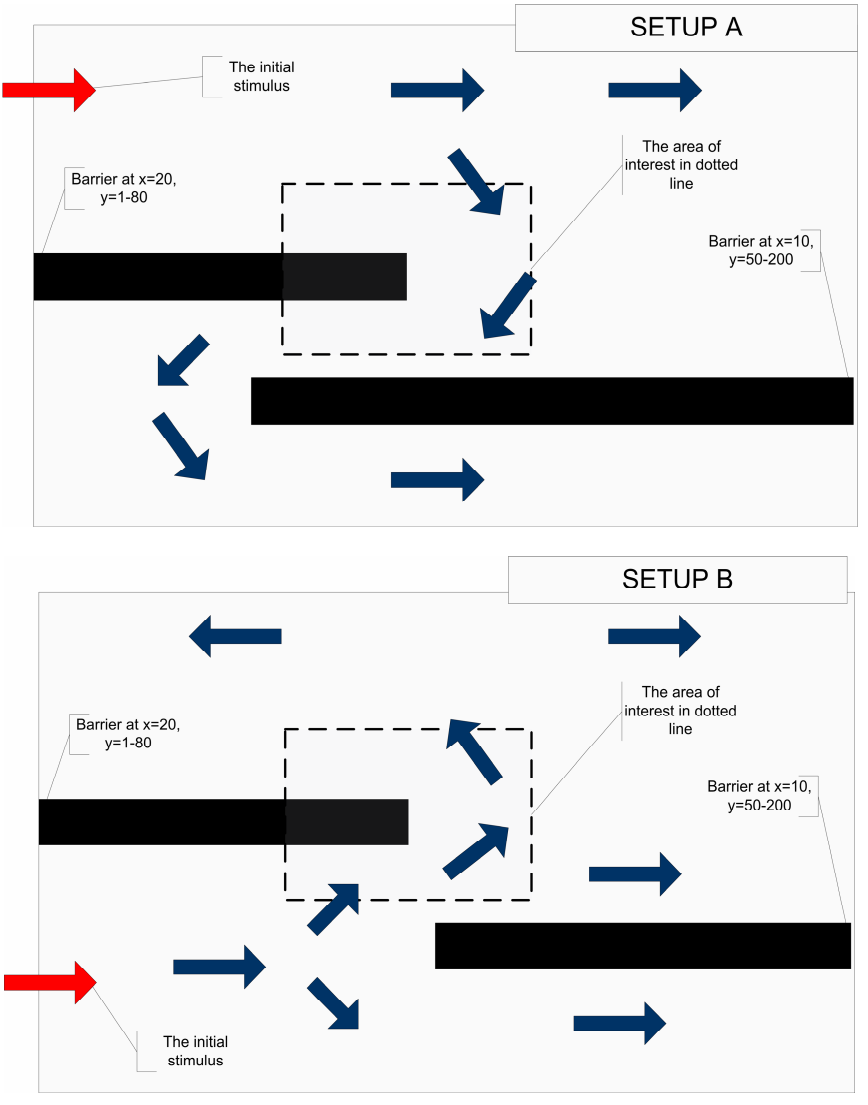

Fig. 1. The two experimental setups used. Both contain areas of heterogeneity

During simulation, transmembrane current was stored for certain grid-points. Activation times were also calculated using transmembrane current criteria analysis. Current waveforms and activation maps were used for comparison with the ones estimated by the methods described in this work.

The two settings used in this paper are shown in Figure 1. Two barriers of scar tissue, cause wavefront to follow a zigzag pathway. Within an area of interest where both areas of normal propagation and velocity changes are present, due to the barriers

of scar tissue, specifically in the rectangle defined by 15<x<25 and 67<y<103, thick recording take place, in a grid, with 10 μm transverse interval and 100μm longitudinal interval, corresponding to one recording per cell.

Regarding implementation issues, simulations were performed with an in-house application written in standard C code, while and post analysis was performed in Matlab.

2.3 Analysis and Features

Having available the calculated data of the simulation setups within the predefined grid, the features depicted for further analysis included the ionic current and the fast kinetic currents, specifically:

- The absolute minimum value of the ionic current, Ion_{min} as a basic morphological feature also strongly affecting the membrane current and the excitability, which is supposed to change due to heterogeneity, and specifically decrease in the infarcted regions.
- Considering the relation between *m*, *h* and *j* fast current kinetic functions, the underlying surfaces of the m-h and h-j plots, i.e. S_{mh} and S_{hj}, as described in Equations 1 and 2 respectively.
- In the same relation, feature D_{mh} describes the minimum distance between m-h curve and (1,1) point, as shown in Figure 2. A similar definition stands for D_{hj} feature (see Equation 3 and 4 for these descriptions).

$$S_{mh} = \frac{\sum_{i=1:N} m(i) \cdot h(i)}{N} \tag{1}$$

$$S_{hj} = \frac{\sum_{i=1:N} h(i) \cdot j(i)}{N} \tag{2}$$

$$D_{mh} = \min\{\sqrt{(m(i)-1)^2 + (h(i)-1)^2}\} \tag{3}$$

$$D_{hj} = \min\{\sqrt{(h(i)-1)^2 + (j(i)-1)^2}\} \tag{4}$$

The reason for selecting these features is to have a close examination at the detailed behavior of each model, especially in heterogeneous areas, instead of the extracellular potentials morphological analysis, usually followed for a more macrospopic analysis and activation times determination.

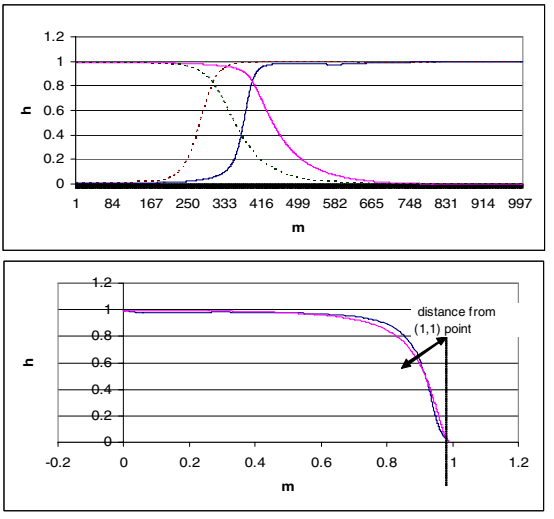

Fig. 2. (top) The voltage-dependent inactivation gate of the fast sodium channel - the h gate and the .fast_sodium_current_m_gate functions. Solid lines BR, dashed lines LR. (down) m-h plots and the distance feature.

3 Results

3.1 Analysis of the Ionic Current

A close examination at the variation of Ion_{min} in the area of interest, which corresponds to an area where the wave is initially planar, then starts rotating until it gets again planar, reveals differences in the behavior of the three models. Near the turning point (20,80), in BR model Ion_{min} decreases, while LR and EJ have an abrupt increase close to the turning point (see Figure 3). Specifically, in setup A, the maximum Ion_{min} value for BR model is at point (25, 62),), at the beginning of the rotation, while point (20,82), just in front of the barrier, holds the maximum Ion_{min} value. In setup B, point (17, 62), at the beginning of the rotation, has the maximum Ion_{min} value, while point (21, 82), just beside the barrier holds the maximum Ion_{min} for LR and EJ models. As shown in Figure 4, the behavior of Ion_{min} in LR-EJ models is quite similar, but quite distinct from that of BR model.

Another way to view possible differences in the area of wavefront rotation, is a representation in polar coordinates (see Figure 5). The different behavior in the areas of rotation is quite obvious. In both setups, the Ion_{min} changes in LR and EJ models in the rotating area seem to be more dependent on the angle. Of course, as expected, in bigger distances from the rotating point, these phenomena decrease.

In order to show the different dependence of Ion_{min} on distance and angle from the rotation point, we have computed a regression model. as shown in Equation 5. The model parameters, as calculated based on the two setups, for the three different models are depicted in Table 1. It has to be noted that the two setups create a

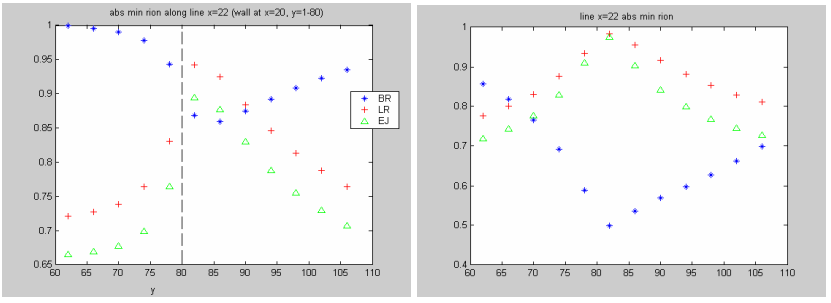

Fig. 3. Along a longitudinal lines (x=22), near the barrier, the evolution of Ion_{min}, normalized to the maximum value within the area of interest, for the 3 models. (left) setup A; (right) setup B.

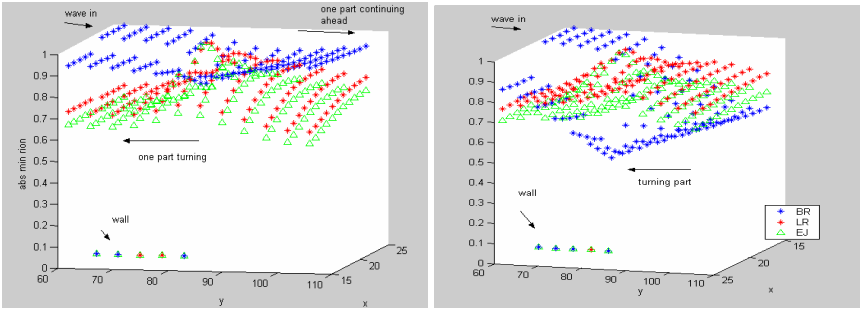

Fig. 4. Normalised Ion_{min} values in the area of interest, in cartesian coordinates, for the three models. (left) setup A, (right) setup B.

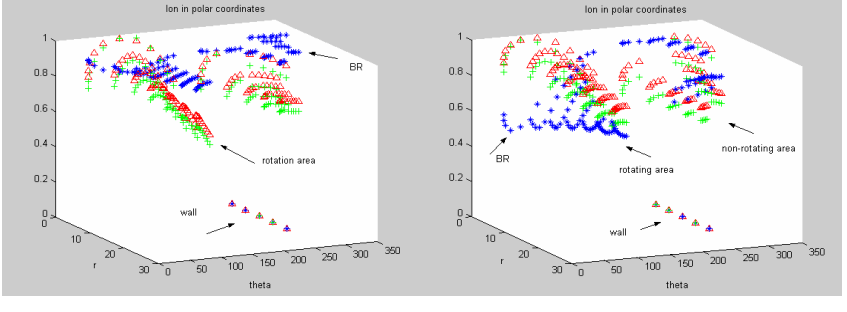

Fig. 5. Normalised Ion_{min} values in the area of interest, in polar coordinates, for the three models. (left) setup A, (right) setup B.

curvature of the opposite side, since propagation follows the opposite direction in the two cases. The difference in the parameter values among the BR model and the other two models are quite obvious.

$$Rion\_min=F(r,theta)= a*r+b*theta+c. \quad (5)$$

Table 1. Linear regression parameters for the relating ionic current with the polar coordinates, for the three models and the two setups

	BR		LR		EJ	
	Setup 1	Setup 2	Setup 1	Setup 2	Setup 1	Setup 2
A (radius)	-0.2330	3.3101	-3.5677	-4.2512	-3.4527	-8.7566
B (theta)	-0.2399	0.6967	-1.6461	-2.6526	-2.2098	-3.1777
C (const)	-115.5088-	236.9449	-224.002	-168.779	-323.035	-193.41

3.2 Analysis of m-h-j Kinetic Functions

m-h Fast Gates Relation

In BR model, D_{mh} increases towards the rotation area, while it decreases again after the rotation towards the normal propagation (see Figure 6). Lowering of Dmh corresponding to more stiff m,h functions, more 0-1 behavior, with less broad transitional area. D_{mh} has the opposite behavior in LR, EJ models, which in general show less variation in D_{mh}. This might imply that LR and EJ kinetics do exhibit the variation expected in varying propagation conditions.

Regarding the surface S_{mh}, again in the turning point there is a significant increase in the BR model, coming back to normal when propagation gets normal, as depicted in Figure 7. There is a similar behavior in LR and EJ models, but with with much lower values.

h-j Inactivation Gates Relation

BR and LR models are quite close, while EJ model has a different behavior, regarding Shj and Dhj. Dhj has much larger values in EJ model (around 0.5) than in BR and LR models. Regarding S_{hj} feature, there are some interesting observations: a) the three models have a distinct behavior, but in general decrease of S_{hj} near the rotation area, and b) there is no axial symmetry as can be seen when comparing S_{hj} in line 22 in the two setups, where the wave is rotating in the opposite direction, as can be seen in Figure 8 (down). This is in contrast with S_{mh}, where there seems to be symmetry.

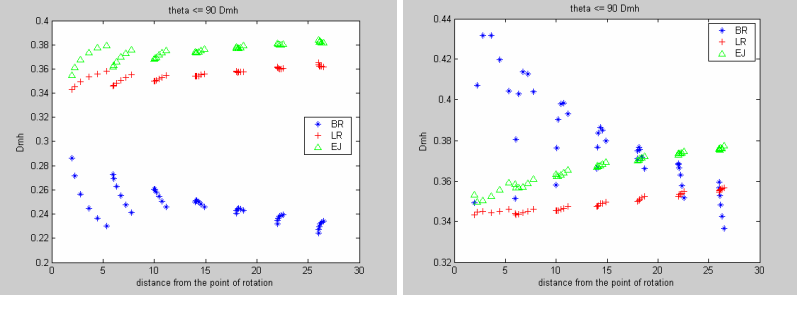

Fig. 6. The D_{mh} feature with distance, for points within the angles 0<theta<90, i.e. in the rotating area. Left setup A, right setup B.

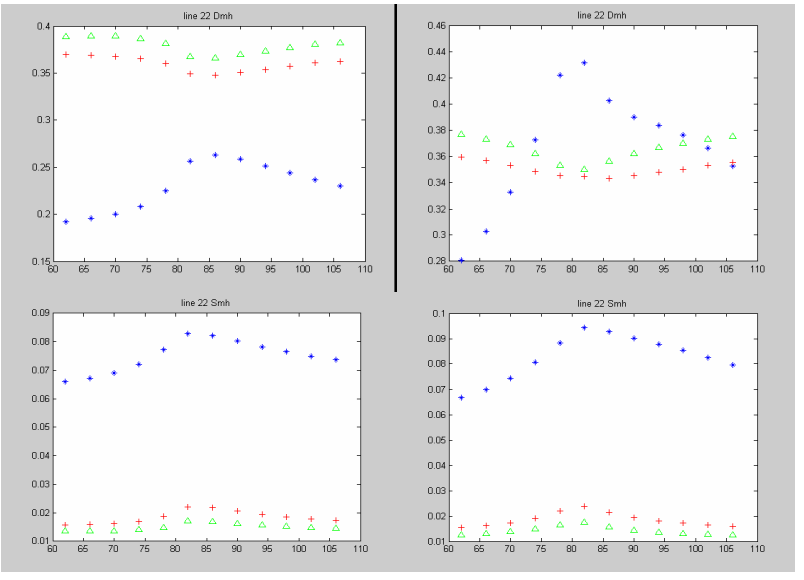

Fig. 7. (Top) The D_{mh} along the longitudinal line x=22. (Down) S_{mh} along the same line. Left setup A, right setup B.

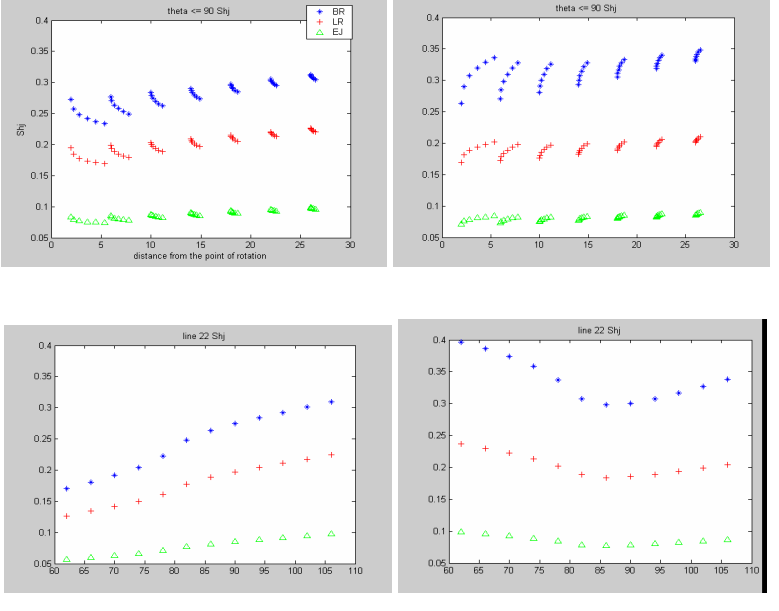

Fig. 8. (Top) The S_{mh} for all point with angle < 90 degrees from th rotating point. (Down) S_{mh} along the longitudinal line x=22. Left setup A, right setup B.

5 Discussion

In the present wok, three different models are used in a 2-D tissue and the differences in the sodium channel kinetics and the ionic currents are studied, for these models and for areas of heterogeneity. The minimum value of the ionic current is a feature found to have different behavior in the BR model than in LR and EJ models. Specifically, in the former it is decreasing, while in the latter it is abruptly increasing in the vicinity of a propagation barrier. In computer simulations of the infarcted myocardial tissue by others [7], LR model has been used, and it is suggested that reduction of the current density of I_{to} found in failing myocytes of human hearts does not seem to contribute significantly to the APD prolongation in heart failure, which instead is mainly due to the enhanced activity of the Na+-Ca2+ exchanger.

Furthermore, regarding the sodium kinetics, and specifically the m-h and the h-j relations in the three models, it was derived that while LR and EJ have a very similar m-h fast kinetics behavior, however quite opposite from the one in BR model, the three models exhibit a distinct behavior as far as h-j relation is concerned, although a reduction in the channel availability is reported in all models. Sodium channel availability, as expressed by the product $h\ j$ of the two inactivation gates (h=fast, j=slow) of I_{Na}., has been studied by [8] and a significant reduction has been reported in the transition zone as compared to the homogeneous segments.

The differences of these models should be checked against experimental evidence, and under different conditions of propagation, in order to understand and evaluate the conditions favorable .for the adoption of each model.

References

1. Beeler, G.W., Reuter, H.: Reconstruction of the action potential of ventricular myocardial fibres. Journal of Physiology 268, 177–210 (1977)
2. Luo, C.H., Rudy, Y.: A dynamic model of the cardiac ventricular action potential. I. Simulation of ionic currents and concentration changes. Circ. Res. 74, 1071 (1994)
3. Ebihara, L., Johnson, E.A.: Fast sodium current in cardiac muscle. A quantitative description. Biophysical Journal 32, 779–790 (1980)
4. Fast, V.G., Kleber, A.G.: Role of wavefront curvature in propagation of cardiac impulse. Cardiovasc Res. 33(2), 258–271 (1997)
5. Maglaveras, N., Offner, F., van Capelle, F.J., Allessie, M.A., Sahakian, A.V.: Effects of barriers on propagation of action potentials in two-dimensional cardiac tissue. A computer simulation study. J Electrocardiol 28(1), 17–31 (1995)
6. Henriquez, C.S., Papazoglou, A.: Using Computer Models to Understand the Roles of Tissue and Membrane Dynamics in Arrhythmogenesis. Proc. IEEE 84(3), 334–354 (1996)
7. Priebe, L., Beuckelmann, D.J.: Simulation study of cellular electric properties in heart failure. Circ Res. 82(11), 1206–1223 (1998)
8. Wang, Y., Rudy, Y.: Action potential propagation in inhomogeneous cardiac tissue: safety factor considerations and ionic mechanism. Am. J Physiol Heart Circ. Physiol 278(4), H1019–H1029 (2000)